

See discussions, stats, and author profiles for this publication at: <https://www.researchgate.net/publication/14672581>

A ligand-induced conformational change in the Yersinia protein tyrosine phosphatase

ARTICLE *in* PROTEIN SCIENCE · SEPTEMBER 1995

Impact Factor: 2.85 · DOI: 10.1002/pro.5560040924 · Source: PubMed

CITATIONS

65

READS

16

5 AUTHORS, INCLUDING:



[Eric Fauman](#)

Pfizer Inc.

28 PUBLICATIONS 2,545 CITATIONS

[SEE PROFILE](#)



[Jeanne Stuckey](#)

University of Michigan

70 PUBLICATIONS 3,845 CITATIONS

[SEE PROFILE](#)



[Jack E Dixon](#)

University of California, San Diego

392 PUBLICATIONS 33,214 CITATIONS

[SEE PROFILE](#)



[Mark A Saper](#)

University of Michigan

55 PUBLICATIONS 9,465 CITATIONS

[SEE PROFILE](#)

A ligand-induced conformational change in the *Yersinia* protein tyrosine phosphatase

HEIDI L. SCHUBERT^{1,2}, ERIC B. FAUMAN¹, JEANNE A. STUCKEY¹,
JACK E. DIXON², AND MARK A. SAPER^{1,2}

¹ Biophysics Research Division and ² Department of Biological Chemistry, The University of Michigan, Ann Arbor, Michigan 48109-1055

(RECEIVED March 29, 1995; ACCEPTED June 14, 1995)

Abstract

Protein tyrosine phosphatases (PTPases) play critical roles in the intracellular signal transduction pathways that regulate cell transformation, growth, and proliferation. The structures of several different PTPases have revealed a conserved active site architecture in which a phosphate-binding loop, together with an invariant arginine, cradle the phosphate of a phosphotyrosine substrate and poised it for nucleophilic attack by an invariant cysteine nucleophile. We previously reported that binding of tungstate to the Yop51 PTPase from *Yersinia* induced a loop conformational change that moved aspartic acid 356 into the active site, where it can function as a general acid. This is consistent with the aspartic acid donating a proton to the tyrosyl leaving group during the initial hydrolysis step. In this report, using a similar structure of the inactive Cys 403 → Ser mutant of the *Yersinia* PTPase complexed with sulfate, we detail the structural and functional details of this conformational change. In response to oxyanion binding, small perturbations occur in active site residues, especially Arg 409, and trigger the loop to close. Interestingly, the peptide bond following Asp 356 has flipped to ligate a buried, active site water molecule that also hydrogen bonds to the bound sulfate anion and two invariant glutamines. Loop closure also significantly decreases the solvent accessibility of the bound oxyanion and could effectively shield catalytic intermediates from phosphate acceptors other than water. We speculate that the intrinsic loop flexibility of different PTPases may be related to their catalytic rate and may play a role in the wide range of activities observed within this enzyme family.

Keywords: conformational change; peptide bond flip; protein tyrosine phosphatases; X-ray crystallography; *Yersinia*

Protein tyrosine phosphatases (PTPases) and protein tyrosine kinases work antagonistically to control the tyrosine phosphorylation levels in many intracellular signal transduction pathways (Fischer et al., 1991; Walton & Dixon, 1993). PTPases have been implicated in cell growth and proliferation, oncogenic transformation, immune cell activation, and hormone receptor signalling. Numerous cDNAs have been cloned that contain a homologous ~260-residue catalytic domain characteristic of PTPases, including the active site consensus sequence HCxxGxGR(S/T) (Zhang & Dixon, 1994). Biochemical evidence and structural diversity of the enzymes suggest that they are localized to different cellular compartments and each may be involved in different signalling pathways.

Recently, the crystal structures of PTPase catalytic domains from *Yersinia* Yop51 and human PTP1B were solved at 2.5 and 2.9 Å resolution, respectively (Stuckey et al., 1994; Barford

et al., 1994). The catalytic regions of the two proteins share only ~20% sequence identity and yet have very similar three-dimensional structures including a highly twisted eight-stranded mixed β-sheet flanked by five α-helices on one side and two on the other. The active site consensus sequence (residues 403–410, *Yersinia* numbering) is located on a reverse turn connecting a β-strand to an α-helix and forms the enzyme's phosphate-binding site or P-loop (red in Fig. 1). Cysteine 403, invariant in all PTPases, is a negatively-charged thiolate (Zhang & Dixon, 1993) that functions as the catalytic nucleophile to form a covalent phosphocysteine intermediate during catalysis (Guan & Dixon, 1991; Cho et al., 1992). Located toward the end of the P-loop, on the first turn of the α-helix, is Arg 409, an invariant arginine that plays key roles in substrate binding and transition state stabilization (Zhang et al., 1994d). The catalytic general acid Asp 356, invariant in all PTPases, is found on a nearby loop, approximately 12 Å from the P-loop in both unliganded *Yersinia* and PTP1B structures.

When tungstate (WO_4^{2-}), a phosphate analog and potent inhibitor of PTPases, was diffused into crystals of human PTP1B,

Reprint requests to: Mark A. Saper, Biophysics Research Division, The University of Michigan, 930 North University Avenue, Ann Arbor, Michigan 48109-1055; e-mail: saper@umich.edu.

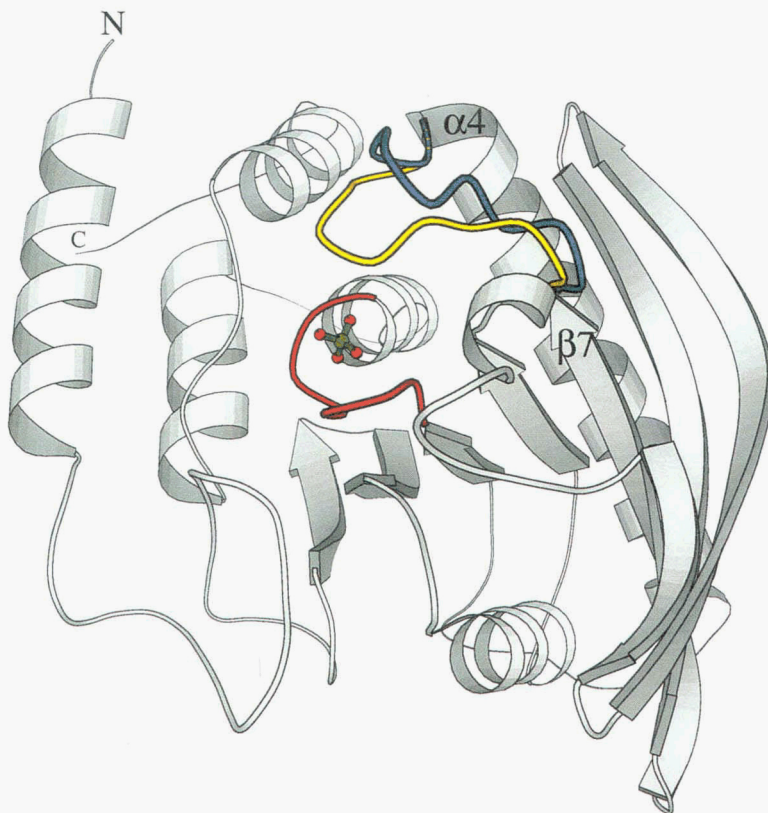


Fig. 1. Schematic drawing depicting the tertiary structure of the *Yersinia* PTPase catalytic domain with sulfate (green) bound at the active site. The active site P-loop of the Cys 403 → Ser enzyme is shown in red. Adjacent to the active site is the WpD loop containing the invariant aspartic acid. The blue loop is the open conformation observed in the unliganded crystal form (Stuckey et al., 1994); in yellow is the closed conformation observed in the sulfate- and tungstate-bound crystal forms. Figure prepared with MOLSCRIPT (Kraulis, 1991).

the anion bound to the P-loop but caused only slight perturbations to active site residues (Barford et al., 1994). In contrast, crystals of the unliganded *Yersinia* PTPase cracked when soaked in tungstate, but enzyme preincubated with 1 mM tungstate yielded crystals of a different space group (Stuckey et al., 1994). Structure determination of this complex revealed that a tetrahedral tungstate anion had bound directly above the thiolate, anchored by hydrogen bonds to main-chain amides of the P-loop (Stuckey et al., 1994). Furthermore, the loop (residues 350–360) containing the catalytic general acid Asp 356 moved up to 6 Å and positioned Asp 356 carboxylate within 3.8 Å of the tungstate oxygen analogous to the O_η phosphoester oxygen of a phosphotyrosine substrate (Stuckey et al., 1994). This suggested that a role for Asp 356 was to protonate the tyrosyl leaving group during the first hydrolysis step of the reaction (Stuckey et al., 1994).

Substrate-induced conformational changes have been described for other phosphotransfer enzymes including hexokinase (Anderson et al., 1979) and triose phosphate isomerase (Sampson & Knowles, 1992). Although such enzymes have comparatively accessible active sites when unliganded, binding of substrate causes a conformational change that positions important functional groups adjacent to the reactants. Furthermore, shielding reactants from bulk solvent can alter the local dielectric constant and allow labile reaction intermediates to form. It can also restrict the accessibility of catalytic intermediates to potential phosphate acceptors so as to favor particular reaction pathways.

The loop conformational change has now been observed in two other *Yersinia* PTPase–oxyanion complexes solved in our laboratory, nitrate and vanadate (E. Fauman, C. Yuvaniyama,

H. Schubert, J. Stuckey, & M. Saper, in prep.; J. Vijayalakshmi & M. Saper, in prep.), a complex of a mutant human PTP1B with a phosphotyrosine-containing peptide (Jia et al., 1995), and a phosphopeptide analog complexed with the *Yersinia* PTPase (J. Stuckey & M. Saper, in prep.). Because the Asp 356-containing loop movement appears critical for PTPase catalysis, this report further describes the conformational change and how it is triggered by binding of oxyanion as illustrated by the structure of an inactive *Yersinia* PTPase mutant, Cys 403 → Ser, containing bound sulfate. We speculate that variability in the amino acid sequence of this important loop may affect its dynamics, and consequently, the catalytic rate of hydrolysis for different PTPases.

Results

WpD loop closes over bound sulfate

The structure of the Cys 403 → Ser mutant of the *Yersinia* PTPase sulfate-bound complex is very similar to that of the wild-type PTPase–tungstate complex (Stuckey et al., 1994) (RMS deviation [RMSD] = 0.28 Å for C_αs), but when superposed on the unliganded *Yersinia* PTPase structure (PDB entry 1YPT) (Stuckey et al., 1994) one prominent conformational difference is observed between residues 351 and 359 (Fig. 2). The two core structures superimpose with an overall RMSD of 0.83 Å for all paired C_αs, but the C_α RMSD for residues 351–359 is 3.6 Å. These residues are located on a surface-accessible loop between β-strand β7 and helix α4, in the vicinity of the active site region (Fig. 1). In contrast to the unliganded structure (blue in Fig. 1), the loop main-chain atoms in the sulfate-bound complex (yellow

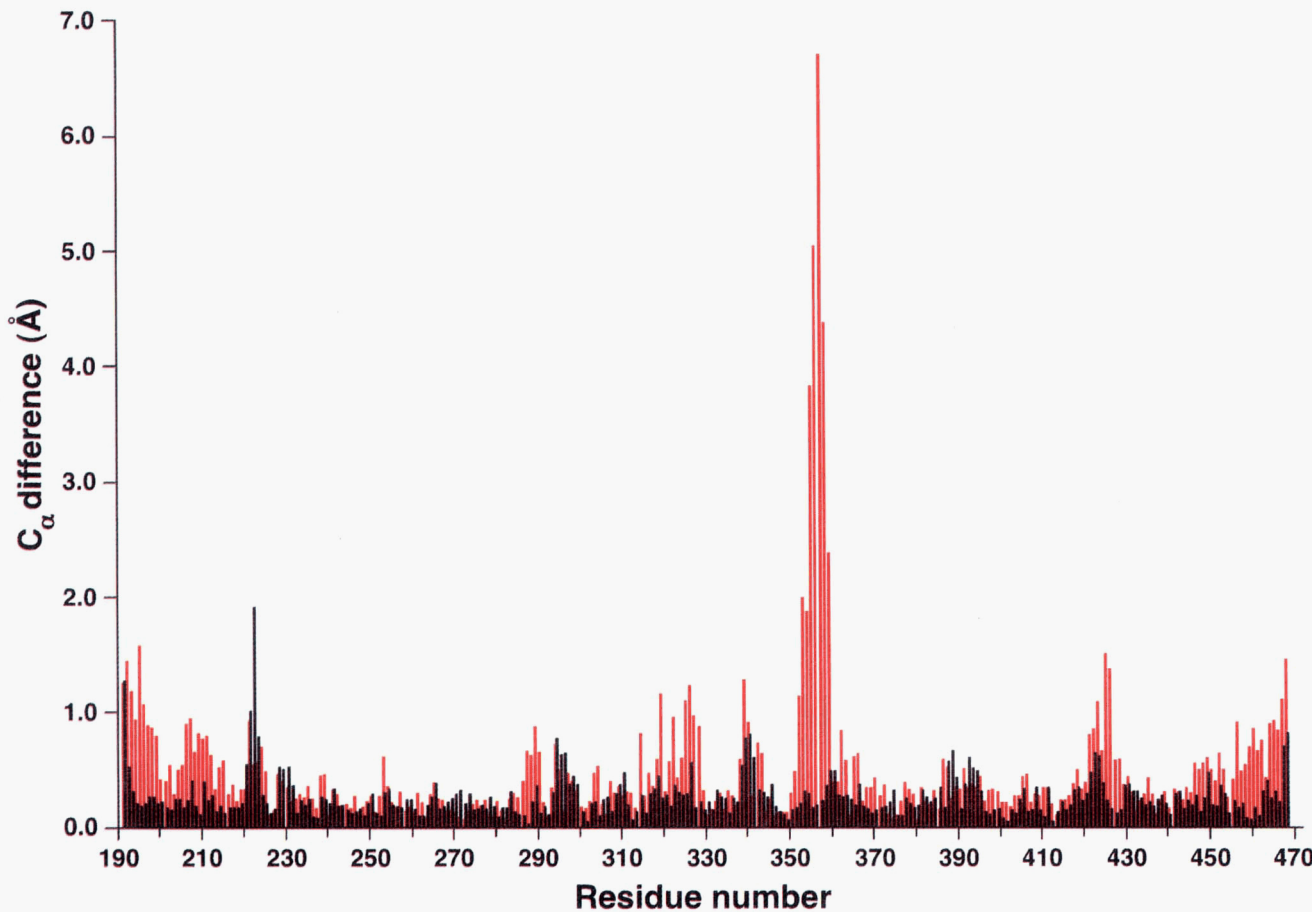


Fig. 2. Deviation (\AA) in α -carbon positions (red) between the unliganded and sulfate-bound superimposed structures of *Yersinia* PTPase. For all α -carbons the RMSD between the native and sulfate-bound structures is 0.83 \AA . Residues 351–359 show a deviation greater than 2σ and represent the only significant conformational change. Shown in black is a similar comparison between the two independent, noncrystallographic symmetry-related molecules in the unliganded crystal's asymmetric unit. These structural differences (RMSD = 0.28 \AA) are primarily due to differences in intermolecular contacts. Because the two unliganded molecules are similar, results have only been presented for one of the molecules in relation to the sulfate-bound crystal structure.

low in Fig. 1) move as much as 7 \AA toward the active site P-loop. The 351–359 loop is referred to here as the WpD loop because it contains the invariant tryptophan, Trp 354, found in all PTPases, the highly conserved Pro 355, as well as the invariant general acid, Asp 356 (Zhang et al., 1994c).

The WpD loop conformational change observed in the PTPase–sulfate complex effectively sequesters the bound anion from bulk solvent (Fig. 3). From model calculations, a sulfate anion positioned in the “open” active site of the unliganded PTPase structure (Fig. 3A) has 10% of its surface (20 \AA^2) accessible to solvent. In the sulfate-bound structure with the “closed” loop conformation (Fig. 3B), only 1% (2 \AA^2) of the oxyanion’s surface area remains solvent accessible. Assuming that the PTPase–sulfate structure is analogous to the structure of an enzyme–product complex, opening of the WpD loop must be required for diffusion of inorganic phosphate out of the catalytic site.

Preliminary studies suggest that the *Yersinia* PTPase only catalyzes phosphoryl transfer to water. Alcohols, such as ethanol or ethylene glycol, are not phosphate acceptors (Z.-Y. Zhang, pers. comm.). This suggests that the WpD loop might close over the active site immediately after the binding of substrate and restrict accessibility of the phosphocysteine enzyme intermediate

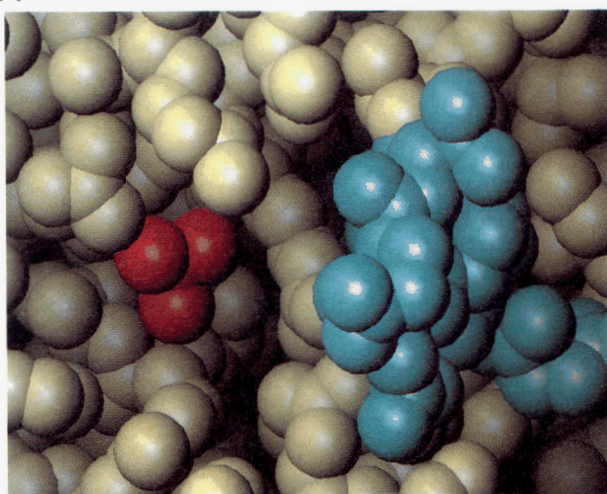
to other nucleophiles besides water. This would prevent the possibility of PTPases functioning as phosphotransferases to other molecules.

To assess the conformational flexibility of the WpD loop, we compared the refined crystallographic temperature factors for the loop residues in the two crystal forms. In the unliganded structure, the mean temperature factor for all atoms in the WpD loop is greater than the temperature factor for the entire protein (25 \AA^2 versus 20 \AA^2). In contrast, the WpD loop in the sulfate-bound structure has a mean *B*-factor lower than the entire protein (15 \AA^2 versus 18 \AA^2 , respectively). This suggests that the WpD loop in the unliganded structure may be more flexible than in the oxyanion-bound structure.

Oxyanion binding and Arg 409 trigger the loop conformational change

The conformational change between the unliganded and oxyanion-bound structures probably originates from small perturbations immediately adjacent to the ligand binding site. Without an oxyanion bound to the P-loop, the Arg 409 side chain is extended and forms two noncoplanar hydrogen bonds with the Glu 290 carboxylate (blue in Fig. 4). Upon anion binding,

A



B

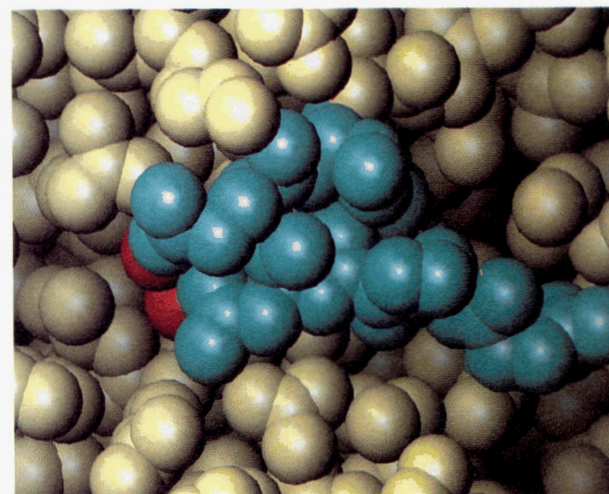


Fig. 3. WpD loop sequesters the bound sulfate from bulk solvent. **A:** The region surrounding the catalytic site in the unliganded *Yersinia* PTPase structure is shown by a CPK space-filling representation. The open conformation of the WpD loop is in aqua. Red spheres indicate where sulfate binds in the sulfate-bound crystal structure. **B:** The sulfate-bound structure showing the WpD loop partially sequestering the sulfate from solvent. In the open conformation, the sulfate has 10% solvent-accessible surface area. Only 1% is accessible in the closed conformation. Solvent-accessible surfaces were calculated with a 1.4-Å radius probe.

the Arg 409 guanidinium group rotates -90° around χ_3 (net RMS movement = 1.8 Å; yellow in Fig. 4) to form a bidentate salt bridge with two of the sulfate oxygens. The Glu 290 carboxylate shifts slightly to form a coplanar salt bridge with Arg 409.

These two side chains, along with three of the sulfate (or phosphate) atoms, form a bicyclic, hydrogen bond network ideal for coordinating the catalytic intermediates (Stuckey et al., 1994; E. Fauman et al., in prep.).

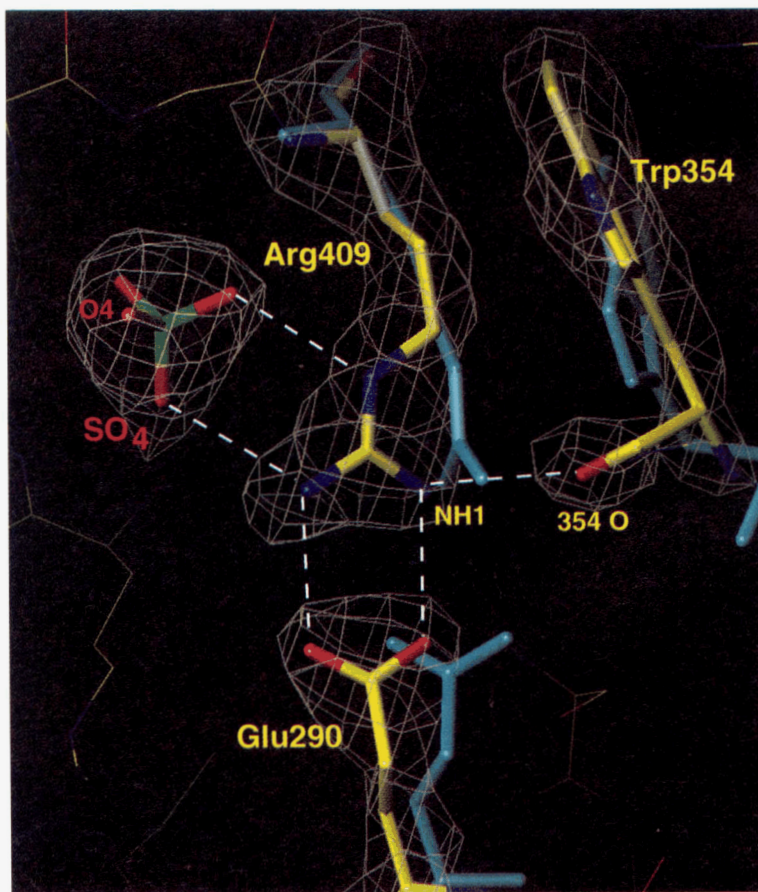


Fig. 4. The active site Arg 409 reorients in response to sulfate binding. Residues near Arg 409 of the unliganded structure are shown in blue and the sulfate-bound structure in yellow. Also shown are contours at 1.2 σ (gold) of a difference Fourier electron density omit map of the sulfate-bound PTPase structure. Omitted from the structure factor calculation were residues Arg 409, Trp 354, Glu 290, and the sulfate. The Arg 409 guanidinium group has rotated 90° around its χ_3 torsion angle. Glu 290 forms bidentate hydrogen bonds with Arg 409. The positioning of Arg 409 is critical for interactions with two oxygens of the bound sulfate. Finally, the binding of sulfate has caused a conformational shift of the WpD loop that results in a new hydrogen bond between Arg 409 N η 1 and the carbonyl of Trp 354.

The small changes in the active site region propagate into larger movements of the WpD loop, especially in residues 354–358. As Arg 409 rotates toward the anion, the adjacent ring of Trp 354 slides 2 Å into a hydrophobic crevice against the protein's central β -sheet (Fig. 5), where it possibly optimizes the van der Waals contacts with the Arg 409 side chain. This movement forces the Trp 354 side chain χ_2 torsion angle from -80° (unliganded structure) to the less optimal -5° angle in the sulfate-bound PTPase structure. The 354–355 peptide bond plane twists and the Trp 354 carbonyl hydrogen bonds to N γ 1 of Arg 409 (distance = 3.0 Å; Figs. 4, 5). The small twist at 354–355 is coupled (via the rigid Pro 355 residue) to movement of an entire β -turn, residues 355–358, toward the active site. The C α of Asp 356 moves 5 Å from its position in the unliganded conformation (Fig. 5) and is positioned 3.5 Å above the Arg 409 guanidinium plane in the sulfate complex (see Fig. 7). If the Arg 409 side chain had not rotated upon oxyanion binding (see above), Asp 356 would be sterically hindered in occupying the position observed in the sulfate complex.

In the unliganded structure, residues 355–358 form a type I β -turn at the center of the WpD loop (Fig. 6A). In the sulfate-bound structure, the peptide bond between Asp 356 and Gln 357 (β -turn residues $i + 1$ and $i + 2$) has flipped into a type II β -turn configuration (Fig. 6B). Although Gln is rarely found at posi-

tion $i + 2$ in type II β -turns (Wilmot & Thornton, 1988), modeling suggests that only with this β -turn conformation can the Asp 356 side chain extend toward the active site. Furthermore, this conformation orients the Gln 357 peptide bond nitrogen so as to hydrogen bond to a water molecule that is trapped in the anion-bound structures (see below).

Asp 356 carboxylate moves greater than 8 Å

The carboxyl group of Asp 356, the proposed general acid (Zhang et al., 1994c), is 12 Å from the oxyanion-binding site in the unliganded *Yersinia* PTPase structure. Upon sulfate binding, the loop conformational change positions the Asp 356 carboxylate O δ 1 atom 3.6 Å from the sulfate oxygen O4, a net movement of 8.4 Å for the carboxylate moiety (Fig. 5).

The Asp 356-sulfate distance of 3.6 Å is too long for a hydrogen bond necessary for direct transfer of a proton from the protonated carboxyl to the substrate's ester oxygen (Fig. 5). This may be an artifact of the crystal's pH. Crystal structures of *Yersinia* PTPase complexed with sulfate or tungstate were solved in precipitants containing 0.1 M Tris-HCl, pH 8.5. The activity of the wild-type enzyme, as measured by k_{cat} , is 1,000-fold less at pH 8.5 than at the pH optimum of 5.0 (Zhang et al., 1994c). Furthermore, at pH 8.5, the solvent-accessible Asp 356

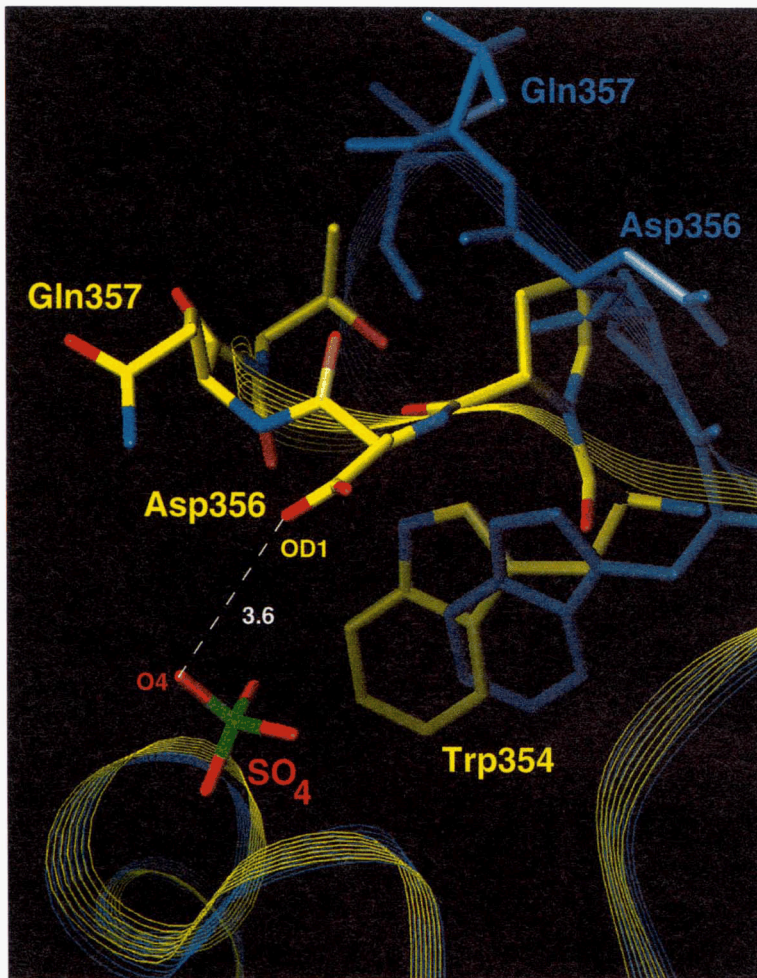


Fig. 5. Conformational change in the WpD loop moves Asp 356 into the active site and 3.6 Å from an oxygen of the bound sulfate. The unbound structure (residues 354–358) is shown in blue and the sulfate-bound structure is shown in yellow with red oxygens and blue nitrogens. The peptide bond between Asp 356 and Gln 357 flips between the two structures forming a type II β -turn in the closed conformation with Gln 357 at the $i + 2$ position. The following is a list of C α shifts between the two forms: Trp 354, 1.9 Å; Pro 355, 3.8 Å; Asp 356, 5.0 Å; Gln 357, 6.7 Å; Thr 358, 4.4 Å.

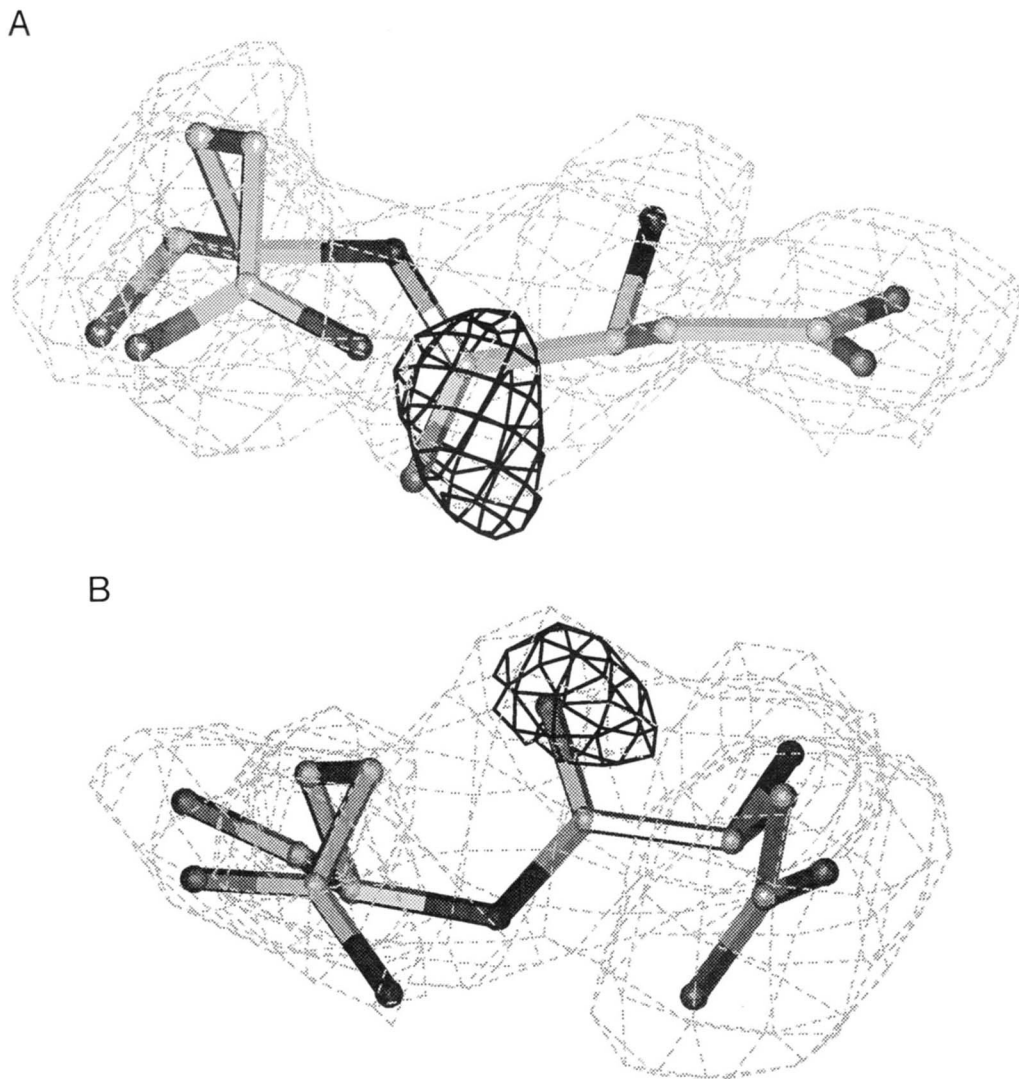


Fig. 6. The peptide bond between residues 356 and 357 changes orientations between unliganded and sulfate-bound structures. Depicted are residues Asp 356 and Gln 357 in (A) the unliganded and (B) the sulfate-bound crystal forms. Superimposed are contours (1σ , dashed grey) of the corresponding $2(F_{obs} - F_{calc})$ final electron density maps. The unliganded WpD loop conformation in A resembles a loose type I β -turn with the following main-chain torsion angles for Asp 356 ($i+1$) and Gln 357 ($i+2$) (ideal values from Wilmut and Thornton [1988] in parentheses): $\phi_{i+1} = -63^\circ$ (-60°), $\psi_{i+1} = -19^\circ$ (-30°); $\phi_{i+2} = -116^\circ$ (-90°), $\psi_{i+2} = -46^\circ$ (0°). The conformation in the sulfate-bound structure (B) is type II with angles $\phi_{i+1} = -53^\circ$ (-60°), $\psi_{i+1} = 143^\circ$ (120°); $\phi_{i+2} = 72^\circ$ (80°), $\psi_{i+2} = 14^\circ$ (0°). To confirm the peptide bond orientations, the occupancy of Asp 356 O was set to zero in each model, and the models were subjected to the simulated-annealing, slow-cool protocol from 1,000 K with X-PLOR. Positive difference density (black contours, 2.0σ in A and 2.5σ in B) calculated with these phases confirmed that the peptide bond had flipped and the β -turn was now in a type II configuration.

($pK_a \approx 5.2$) would be predominantly deprotonated, and charge repulsion would prevent it from approaching the negatively charged sulfate oxygen closer than van der Waals distance.

In support of the explanation that the Asp 356 scissile oxygen distance is regulated by pH, we note that the two crystal structures of a bovine low molecular weight PTPase (LMW PTPase) have been solved at different pHs (Su et al., 1994; Zhang et al., 1994a). Though the primary sequence and topology of these enzymes are very different from *Yersinia* PTPase (Stuckey et al., 1994) and human PTP1B (Barford et al., 1994), the LMW PTPase has comparable secondary structure elements and a conserved active site P-loop that contains the invariant

Cys and Arg residues (Zhang et al., 1994d). Both LMW PTPase structures reveal that Asp 129, recently shown to be important for catalysis (Taddei et al., 1994; Zhang et al., 1994b), is pointed toward the bound oxyanion. In one structure, solved at pH 7.5 with bound phosphate (Zhang et al., 1994a), the Asp 129 carboxylate oxygen is 3.8 Å from the phosphate oxygen. In the other structure solved at pH 5.5 with bound sulfate (Su et al., 1994), this distance shortens to 2.7 Å. This pH-dependent trend suggests that, at lower and catalytically more optimal pH, the *Yersinia* PTPase Asp 356 carboxyl group would form a hydrogen bond (<3.0 Å) to the bound anion, and analogously, donate a proton directly to the leaving group oxygen of a suitable

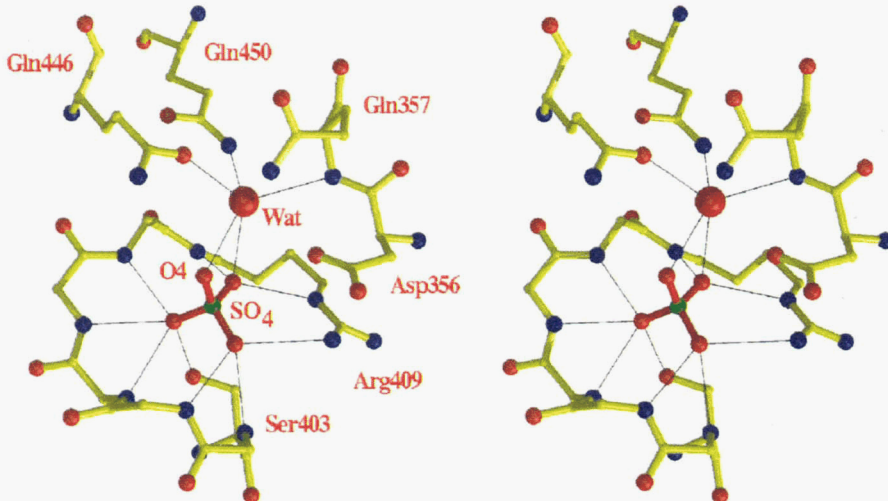


Fig. 7. A water molecule trapped in the active site of the sulfate-bound structure bridges the closed WpD loop and the bound oxyanion. The water molecule is within 3.3 Å of several residues including the sulfate. Distances from the water are: 3.0 Å to sulfate oxygen O4 that is analogous to the scissile ester linkage of phosphotyrosine, 2.7 Å to sulfate oxygen O2, 3.2 Å to Gln 446 Nε1, 3.3 Å to Gln 450 Nε2, and 3.0 Å to the amide of Gln 357 on the WpD loop. The carboxyl side chain of Asp 356 is 3.5 Å from the water and 3.6 Å from sulfate O4.

substrate. To test this hypothesis, we have energy-minimized (XPLOR) a model of a *Yersinia* PTPase–phosphotyrosine complex and shown that a protonated Asp 356 can form a hydrogen bond with the scissile oxygen without perturbing the observed conformation of the WpD loop (E. Fauman, C. Yuvaniyama, H. Schubert, J. Stuckey, & M. Saper, in prep.).

Water molecule trapped in the active site after loop closure

The structure of the sulfate-bound PTPase contains a well-resolved water molecule “trapped” between the closed WpD loop and the anion-binding site (Fig. 7). The water is within hydrogen bonding distance (<3.3 Å) of the side chains of the invariant residues Gln 446 and Gln 450, the sulfate oxygens O2 and O4, and the main-chain nitrogen of Gln 357 on the WpD loop. We do not believe that this is the water molecule that acts as the nucleophile during hydrolysis of the phosphocysteine (Enz-S-PO₃²⁻) intermediate. Assuming an in-line mechanism, we expect that the nucleophilic water would attack the phosphate from a direction directly opposite the phosphorus–sulfur bond (Zhang et al., 1994d). In the sulfate-bound structure this position is already occupied by sulfate oxygen O4. Because the “trapped” water molecule is inaccessible to bulk solvent and is coordinated by two conserved glutamine residues, we propose that this water plays a critical structural role in catalysis by hydrogen bonding to the catalytic intermediates.

Discussion

Influence of crystal packing on WpD loop conformation

Though we have described the loop movement as a transition between two distinct conformations, the loop in solution is likely very flexible, especially without a bound oxyanion. The open WpD loop conformation observed in the unliganded crystal form is probably one of many that exist in solution but has been selected by crystal packing. Further evidence comes from a recent structure determination at 3.0 Å resolution of a slightly different unliganded crystal form of the *Yersinia* PTPase grown in the presence of sodium acetate and sodium citrate (J.

Vijayalakshmi & M. Saper, unpubl. data). These crystals have similar cell dimensions to the previously described unliganded crystals (Stuckey et al., 1994) but are of space group *P*3₂1 rather than *P*3₂. The WpD loop in this new structure is clearly intermediate between the two forms described here but is more similar to the unliganded form. The Arg 409 and Trp 354 side chains are positioned as in the original unliganded crystals. There is no evidence of a molecule bound to the P-loop at a position analogous to the sulfate or tungstate site.

Although the WpD loop conformations in both unliganded crystal forms are stabilized by contacts with adjacent symmetry-related molecules (data not shown), movement of the WpD loop is not prevented by crystal packing. Consequently, when unliganded crystals are soaked in stabilizing solutions containing sodium tungstate, or low concentrations of heavy atom compounds containing oxyanions such as nitrate or phosphate, the crystals crack within hours. The anion has presumably bound to the active site, forced the WpD loop to close, and disrupted any crystal lattice contacts between the loop and adjacent molecules.

WpD loop flexibility and enzyme activity

Using the common substrate *p*-nitrophenylphosphate, the protein tyrosine phosphatases characterized so far show a wide range of catalytic activity (Zhang & Dixon, 1994). By far the most efficient PTPase—more than 100-fold faster than any mammalian enzyme—is from *Yersinia*, the causative bacterium of bubonic and pneumonic plague. The enzyme’s high catalytic rate ($k_{cat} = 1,230 \text{ s}^{-1}$), rather than substrate specificity, is presumably responsible for the pathogen’s ability to suppress the host immune system. In contrast, eukaryotic PTPases involved in normal signal transduction are usually much slower ($k_{cat} \approx 1-50 \text{ s}^{-1}$), perhaps to insure that cellular levels of phosphotyrosine are precisely maintained. The consequences of perturbing PTPase catalytic rate emphasize the importance of understanding catalytic mechanisms and how structural features control catalytic rate.

Our results suggest that conformational flexibility of the WpD loop in the *Yersinia* PTPase is necessary for efficient catalysis. Loop closure is essential during the first hydrolysis step so that

Asp 356 can protonate the leaving group and sequester the phosphocysteine intermediate. Opening of the loop is necessary for release of product and binding of new substrate. Because all PTPases may require the functionality of a general acid for efficient hydrolysis (Taddei et al., 1994; Zhang et al., 1994b; Zhang & Dixon, 1994; Denu et al., 1995), we hypothesize that the energy barrier of WpD loop opening/closing could have significant effects on the kinetics of all PTPases.

Alignment of WpD loop sequences from a range of divergent PTPases (Fig. 8) shows that residues surrounding the highly conserved Trp-Pro-Asp sequence are variable. The residue immediately following the invariant Asp (Gln 357 in the *Yersinia* PTPase) is usually Phe or His in mammalian phosphatases, or Met or Ser in the yeast PTPases (Fig. 8). The Gln 357 C_α moves 7 Å between the unliganded and liganded *Yersinia* PTPase structures. Furthermore, Gln 357 is residue *i* + 2 of a β-turn and adjacent to the 356–357 peptide bond, which is observed to flip when the β-turn switches between type I and type II configurations (see Results). Side chains other than glycine or asparagine are rarely found in the *i* + 2 position of a type II β-turn due to steric clashes with the peptide carbonyl (Wilmot & Thornton, 1988). If the peptide bond orientations observed in the *Yersinia* PTPase structure typify other PTPase structures, we might expect the identity of the residue 357 side chain to affect the energy barrier required to flip the 356–357 peptide bond into the type II configuration, and thus, the rate of loop movement.

WpD loop closure and catalytic rate may also be influenced by substrate binding. Though *Yersinia* PTPase displays loop closure when oxyanion alone is bound, other PTPases may require that other portions of the substrate in addition to the phosphate moiety (such as the phosphotyrosine ring, adjacent side-chain or main-chain atoms) make interactions with residues of the WpD loop to promote closure. The recently solved human PTP1B structure (Barford et al., 1994) may be such an example. Unlike *Yersinia*, both unliganded and tungstate-bound PTP1B structures have WpD loop conformations similar to the open form observed in the *Yersinia* unliganded structure. Crystal packing constraints may have prevented loop closure from occurring in the PTP1B-tungstate complex. An alternative explanation is that phenylalanine at residue 182 of the PTP1B WpD loop (structurally equivalent to the *Yersinia* Gln 357) may

make the loop more resistant to closure as argued above. Interestingly, when phosphotyrosine was soaked into unliganded crystals of a mutant PTP1B, the analogous WpD loop in PTP1B (residues 179–187) did undergo a conformational change similar to that observed in the *Yersinia*-oxyanion complexes (Jia et al., 1995). Phe 182 of PTP1B makes hydrophobic interactions with the phenyl ring of the phosphotyrosine substrate that likely stabilizes the “closed” conformation.

Materials and methods

Crystallization

The catalytic domain (residues 163–468) of Yop51, a PTPase from *Yersinia enterocolitica*, was expressed, purified, and characterized as previously described (Zhang et al., 1992). Trigonal crystals of the unliganded wild-type enzyme (space group *P*3₂, two molecules per asymmetric unit) were grown by vapor diffusion against reservoirs containing 10–12% polyethylene glycol 1500, 10% 2-methyl-2,4-pentanediol, 0.1% 2-mercaptoethanol, and 1 mM imidazole, pH 7.2 (Stuckey et al., 1994). These crystals cracked when soaked in stabilizing solutions containing even submillimolar concentrations of phosphate analogs, such as tungstate or sulfate. By premixing the wild-type enzyme with 1 mM sodium tungstate ($K_D = 61 \mu\text{M}$ [Zhang et al., 1994d]), we grew an orthorhombic crystal form of the liganded enzyme (Stuckey et al., 1994).

A catalytically inactive mutant of the *Yersinia* PTPase catalytic domain, with the essential nucleophile Cys 403 mutated to serine (Cys 403 → Ser) (Guan & Dixon, 1990), formed crystals in the presence of lithium sulfate (Li₂SO₄) that were isomorphous to those of the PTPase-tungstate complex (Stuckey et al., 1994). Equal volumes of protein (10–12 mg/mL in 30 mM NaCl, 5 mM Na acetate, pH 5.7) and precipitant (18–22% w/v polyethylene glycol 4000, 200 mM Li₂SO₄, 5% 2-propanol, 0.1% 2-mercaptoethanol, 100 mM Tris-HCl, pH 8.5) were mixed and equilibrated by vapor diffusion against 1 mL of the same precipitant. The rectangular, platelike crystals (0.6 × 0.3 × 0.05 mm) were of space group *P*2₁2₁2₁ and had unit cell dimensions of $a = 56.4 \text{ \AA}$, $b = 49.8 \text{ \AA}$, $c = 100.8 \text{ \AA}$ with one molecule per asymmetric unit.

Structure solution

Diffraction images for the orthorhombic tungstate and sulfate complex crystals were collected at room temperature on an SDMS multiwire area detector system (Hamlin, 1985; Howard et al., 1985) mounted on a Rigaku RU-200 rotating anode generator (50 kV, 100 mA). Reflections were indexed and integrated by the programs MADNES and PROCOR (Messerschmidt & Pflugrath, 1987; Kabsch, 1988), and batches of ~500 reflections each were scaled to each other with XSCALE (Kabsch, 1988). Data statistics are shown in Table 1.

The site of bound tungstate in the wild-type PTPase-tungstate complex was located by calculating a difference Patterson map (PROTEIN [Steigemann, 1974]) using the sulfate-containing Cys 403 → Ser mutant crystal data as “native.” A second derivative, prepared by soaking the Cys 403 → Ser mutant crystals in stabilizing solution containing 5 mM *p*-chloromercuribenzyl-sulfonic acid in the absence of 2-mercaptoethanol, was confirmed by difference Fourier maps phased with the single tungstate derivative site (PHASES [Furey & Swaminathan, 1990]). Maps cal-

<i>Yersinia</i> Yop51	350 H V G N W P D Q T A V P	361	
Yeast PTP1	215 Y F D L W K D M	N K P	225
Yeast PTP2	600 Q Y K N W L D S C G V D		611
Human PTP1B	175 H Y T T W P D F	G V P	185
Human T-Cell	177 H Y T T W P D F	G V P	187
Human PTP1C	416 Q Y L S W P D H	G V P	426
Rat LAR (domain 1)	470 Q F M A W P D H	G V P	480
Human PTPmegal	815 Q Y I A W P D H	G V P	825
Human PTP PEP	189 H Y K N W P D H	D V P	199

Fig. 8. Amino acid sequence alignment of the WpD loop region (residues 350–361 in the *Yersinia* PTPase) from representative divergent PTPases. Alignment adapted from Zhang et al. (1994c). See Zhang et al. (1994c) for references to amino acid sequences.

Table 1. Diffraction data and multiple isomorphous replacement phasing statistics for Cys 403 → Ser mutant of the *Yersinia* PTPase complexed with sulfate

Compound	Resolution (Å)	No. of unique reflections	Completeness (%)	R_{sym}^a (%)	R_{iso}^b (%)	No. of sites	Figure of merit	Phasing power ^c
Native	2.5	9,156	92	8.2				
Na ₂ WO ₄ (1 mM, co-crystallized with wild-type enzyme)	2.8	5,937	85	11.1	18.1	1	0.452	1.71
<i>p</i> -chloromercuribenzylsulfonic acid (5 mM, 24-h soak)	3.0	4150	70	12.5	24.1	1	0.309	1.43
Overall mean figure of merit (10–2.8 Å) = 0.545								

$$^a R_{sym} = \sum_{hkl} \sum_i |I_i - \langle I \rangle| / \sum \langle I \rangle$$

$^b R_{iso} = \sum (|F_P - F_{PH}|) / \sum F_P$, where F_P and F_{PH} are the structure factors of the native protein and protein complexed with heavy atom, respectively.

c Phasing power is defined as (RMS F_H)/(RMS lack of closure error), where F_H is the heavy atom structure factor.

culated from multiple isomorphous replacement phases derived from the two derivatives were solvent flattened (Wang, 1985) (assuming 40% solvent) in PHASES (Furey & Swaminathan, 1990).

A partial polyalanine chain of the sulfate-bound PTPase structure was built into these maps with the molecular graphics program O (version 5.9.1 [Jones et al., 1991]). Intermediate models were minimized with XPLOR (Brünger, 1993), and calculated phases were phase-combined with the MIR probabilities using the program SIGMAA (Read, 1986) to improve the interpretability of the electron density. Difference electron density maps calculated with coefficients ($F_{obs} - F_{calc}$), α_{calc} revealed a $>5\sigma$ positive density peak near the anion-binding P-loop that was consistent with a bound sulfate anion (SO_4^{2-}). The sulfate-bound structure was refined by alternating cycles of model rebuilding and the simulated annealing (1,000 K)/slow-cool minimization protocol of XPLOR (Brünger, 1993) to a final R -factor of 17.4% (9,156 reflections, 92% complete between 10 and 2.5 Å). The structure has RMS bond and angle deviations from ideality of 0.02 Å and 3.7°, respectively, and contains 2,228 non-hydrogen atoms, 285 residues (191–468), 63 water molecules, and 2 sulfate anions. As in the unliganded trigonal crystal form, there is no interpretable electron density in this crystal form for the amino-terminal residues 163–190 and we presume they are disordered in the crystal. Crystallographic coordinates have been deposited in the Brookhaven Protein Data Bank (Bernstein et al., 1977) as entry 1YTS.

A sulfate anion binds to the mutant PTPase at a position similar to that of the tungstate ion in the wild-type PTPase-tungstate complex and assumably mimics the enzymatic product, inorganic phosphate. There are no notable differences in the protein structure caused by the substitution of serine for the catalytic cysteine. The sulfate sulfur is 3.4 Å from the Ser 403 Oγ comparable to the tungsten–Cys 403 Sγ distance of 3.5 Å in the tungstate complex. In both oxyanion-bound crystal structures, a second sulfate is liganded to several residues, nonconserved in other PTPases, and located distant from the active site at the C-terminal end of the long α-helix, α4.

Structure comparisons

The unliganded native (Stuckey et al., 1994) (Protein Data Bank entry 1YPT) and sulfate-bound structures were superimposed

by a published protocol (Perry et al., 1990). Residues of the two structures were defined as part of the core if their Cαs were within 10 Å of another core Cα and had intramolecular distances to other core residues that did not vary between the two structures by more than 0.5 Å. The core consisted of 131 residues out of the 277 residues common to both structures. The superposition matrix was determined by least-squares minimization of the distances between corresponding Cαs of the core residues (results shown in Fig. 2). Because two similar molecules are present in the asymmetric unit of the unliganded crystal form, comparisons of only one of the unliganded molecules with the sulfate-bound crystal structure is presented.

Acknowledgments

We thank Dr. Zhong-Yin Zhang for discussions. Research funding provided by the National Institutes of Health (AI34095 to M.A.S. and DK18849 to J.E.D.), The University of Michigan Multipurpose Arthritis Center (M.A.S.), American Cancer Society (J.A.S.), and the Walther Cancer Institute (J.E.D.). H.L.S. is a Joe Dawson Fellow of the Walther Cancer Institute. M.A.S. is a Pew Scholar in the Biomedical Sciences.

References

- Anderson CM, Zucker FH, Steitz TA. 1979. Space-filling models of kinase clefts and conformation changes. *Science* 204:375–380.
- Barford D, Flint AJ, Tonks NK. 1994. Crystal structure of human protein tyrosine phosphatase 1B. *Science* 263:1397–1404.
- Bernstein FC, Koetzle TF, Williams GJB, Meyer EF Jr, Brice MD, Rodgers JR, Kennard O, Shimanouchi T, Tasumi M. 1977. The Protein Data Bank: A computer-based archival file for macromolecular structures. *J Mol Biol* 112:535–542.
- Brünger TA. 1993. *XPLOR version 3.1 manual*. New Haven, Connecticut: Yale University Press.
- Cho H, Krishnaraj R, Kitas E, Bannwarth W, Walsh CT, Anderson KS. 1992. Isolation and structural elucidation of a novel phosphocysteine intermediate in the LAR protein tyrosine phosphatase enzymatic pathway. *J Am Chem Soc* 114:7296–7298.
- Denu JM, Zhou G, Guo Y, Dixon JE. 1995. The catalytic role of aspartic acid-92 in the human dual specificity PTPase, VHR. *Biochemistry* 34:3396–3403.
- Fischer EH, Charbonneau H, Tonks NK. 1991. Protein tyrosine phosphatases: A diverse family of intracellular and transmembrane enzymes. *Science* 253:401–406.
- Furey W, Swaminathan S. 1990. PHASES—A program package for the processing and analysis of diffraction data from macromolecules. *Am Crystallogr Assoc Meeting Abstr* 18:73.
- Guan KL, Dixon JE. 1990. Protein tyrosine phosphatase activity of an essential virulence determinant in *Yersinia*. *Science* 249:553–556.
- Guan KL, Dixon JE. 1991. Evidence for protein-tyrosine-phosphatase ca-

- talysis proceeding via a cysteine-phosphate intermediate. *J Biol Chem* 266:17026–17030.
- Hamlin R. 1985. Multiwire area X-ray diffractometers. *Methods Enzymol* 114:416–452.
- Howard AJ, Nielsen C, Xuong NH. 1985. Software for a diffractometer with multiwire area detector. *Methods Enzymol* 114:452–472.
- Jia Z, Barford D, Flint AJ, Tonks NK. 1995. Structural basis for phosphotyrosine peptide recognition by protein tyrosine phosphatase 1B. *Science* 268:1754–1758.
- Jones TA, Zou JY, Cowan SW, Kjeldgaard M. 1991. Improved methods for building protein models in electron density maps and the location of errors in these models. *Acta Crystallogr A* 47:110–119.
- Kabsch W. 1988. Evaluation of single-crystal X-ray diffraction data from a position-sensitive detector. *J Appl Crystallogr* 21:916–924.
- Kraulis PJ. 1991. MOLSCRIPT: A program to produce both detailed and schematic plots of protein structure. *J Appl Crystallogr* 24:946–950.
- Messerschmidt A, Pflugrath JW. 1987. Crystal orientation and X-ray pattern prediction routines for area-detector diffractometer systems in macromolecular crystallography. *J Appl Crystallogr* 20:306–315.
- Perry KM, Fauman EB, Finer-Moore JS, Montfort WR, Maley GF, Maley F, Stroud RM. 1990. Plastic adaptation toward mutations in proteins: Structural comparison of thymidylate synthases. *Proteins Struct Funct Genet* 8:315–333.
- Read RJ. 1986. Improved Fourier coefficients for maps using phases from partial structures with errors. *Acta Crystallogr A* 42:140–149.
- Sampson NS, Knowles JR. 1992. Segmental movement: Definition of the structural requirements for loop closure in catalysis by triosephosphate isomerase. *Biochemistry* 31:8482–8487.
- Steigemann W. 1974. Die Entwicklung und Anwendung von Rechenverfahren und Rechenprogrammen zur Strukturanalyse von Proteinen am Beispiel des Trypsin-Trypsininhibitor Komplexes, des freien Inhibitors und der L-Asparaginase. Ph.D. Thesis, Technische Universität, Munich.
- Stuckey JA, Schubert HL, Fauman EB, Zhang ZY, Dixon JE, Saper MA. 1994. Crystal structure of *Yersinia* protein tyrosine phosphatase at 2.5 Å and the complex with tungstate. *Nature* 370:571–575.
- Su XD, Taddei N, Stefani M, Ramponi G, Nordlund P. 1994. The crystal structure of a low-molecular-weight phosphotyrosine protein phosphatase. *Nature* 370:575–578.
- Taddei N, Chiarugi P, Cirri P, Fiaschi T, Stefani M, Camici G, Raugei G, Ramponi G. 1994. Aspartic-129 is an essential residue in the catalytic mechanism of the low M_r phosphotyrosine protein phosphatase. *FEBS Lett* 350:328–332.
- Walton KM, Dixon JE. 1993. Protein tyrosine phosphatases. *Annu Rev Biochem* 62:101–120.
- Wang BC. 1985. Resolution of phase ambiguity in macromolecular crystallography. *Methods Enzymol* 115:90–112.
- Wilmot CM, Thornton JM. 1988. Analysis and prediction of the different types of beta-turn in proteins. *J Mol Biol* 203:221–232.
- Zhang M, Van Etten RL, Stauffacher CV. 1994a. Crystal structure of bovine heart phosphotyrosyl phosphatase at 2.2-Å resolution. *Biochemistry* 33:11097–11105.
- Zhang Z, Harms E, Van Etten RL. 1994b. Asp 129 of low molecular weight protein tyrosine phosphatase is involved in leaving group protonation. *J Biol Chem* 269:25947–25950.
- Zhang ZY, Clemens JC, Schubert HL, Stuckey JA, Fischer MW, Hume DM, Saper MA, Dixon JE. 1992. Expression, purification, and physicochemical characterization of a recombinant *Yersinia* protein tyrosine phosphatase. *J Biol Chem* 267:23759–23766.
- Zhang ZY, Dixon JE. 1993. Active site labeling of the *Yersinia* protein tyrosine phosphatase: The determination of the pK_a of the active site cysteine and the function of the conserved histidine 402. *Biochemistry* 32:9340–9345.
- Zhang ZY, Dixon JE. 1994. Protein tyrosine phosphatases: Mechanism of catalysis and substrate specificity. *Adv Enzymol Relat Areas Mol Biol* 68:1–36.
- Zhang ZY, Wang Y, Dixon JE. 1994c. Dissecting the catalytic mechanism of protein-tyrosine phosphatases. *Proc Natl Acad Sci USA* 91:1624–1627.
- Zhang ZY, Wang Y, Wu L, Fauman EB, Stuckey JA, Schubert HL, Saper MA, Dixon JE. 1994d. The Cys(X)₅Arg catalytic motif in phosphoester hydrolysis. *Biochemistry* 33:15266–15270.